

# Linear Model of a Novel 5-Phase Segment Type Switched Reluctance Motor

D. Uygun<sup>1</sup>, G. Bal<sup>2</sup>, I. Sefa<sup>2</sup>

<sup>1</sup>Enturk Energy Inc.Co., Gazi University, Technoplaza, BB12-B,  
Golbasi 06830, Ankara, Turkey

<sup>2</sup>Department of Electrics Electronics Engineering, Faculty of Technology, Gazi University,  
Teknikokullar, Besevler 06590, Ankara, Turkey  
durmus.uygun@enturkenerji.com

**Abstract**—This paper introduces the general linear magnetic circuit model of a novel 5-phase segment type switched reluctance motor (ST-SRM) of which rotor cores are embedded in an aluminum block as well as to improve the performance characteristics under simultaneous two-phase (bipolar) excitation of windings. The developed model implements the magneto motor force (mmf) that is necessary to produce short and exclusive magnetic flux paths minimizing the commutation switching and eddy current losses in the laminations. For this purpose, an equivalent magnetic circuit for newly developed ST-SRM and the underlying assumptions are given. The concept of apparent inductance and torque equations of two-phase simultaneously excited ST-SRM is introduced and the effectiveness and deficiencies of the linear model are given.

**Index Terms**—Magnetic circuit model, switched reluctance, segmental rotor, two phase excitation.

## I. INTRODUCTION

Due to rapid developments in semi-conductor technology, thereby producing semi-conductor packages such like IGBTs and MOSFETs, switched reluctance motors attracted much more considerable attention throughout the industrial environment. Whilst the SRM has a simple operating principle, it is really difficult to design and develop performance predictions for these kinds of motor. This is due to the nonlinear magnetic characteristics of the machine under normally saturated operation. Due to the winding arrangement in the conventional SRM as seen Fig. 1, mutual coupling between phases is generally neglected [1]. Phase flux linkage depends only on the rotor position and the current in the phase of interest; the phases are taken to be magnetically independent [2]. But in contrast, the mutually coupled SRM phases under simultaneous two-phase (bipolar) excitation of windings, especially for SRMs consisting of segmental rotors, are magnetically coupled and the flux linkage functions are resulted from rotor position and the currents in adjacent phases which are simultaneously excited.

In this study, the magnetic circuit model for designed 5-phase segment type SRM (ST-SRM) with short-pitched

windings are presented [3] in order to determine the flux linkage of each phase for rotor position and combination of phase currents. The linear model of ST-SRM is formed by considering the machine dimensions. The linear model of ST-SRM makes the prediction of torque, inductance and instantaneous phase fluxes despite the fact that the magnetic nonlinearity is neglected. Besides, by taking into account concept of apparent inductance [4]; simulation of conventional 5-phase SRM and newly designed 5-phase segment type SRM having the same main motor dimensions such as stator outer diameter, rotor outer diameter, stack length, air gap length, etc. are performed. Consequently, the torque variations of each machine are compared to verify that the ST-SRM can produce higher torque than the conventional one.

## II. MACHINE MODELS

In order to carry out necessary analytical calculations and simulations, two different machine models are considered.

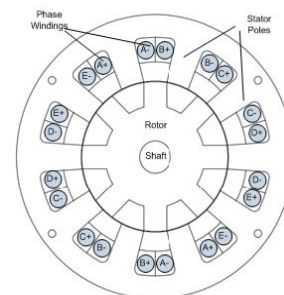


Fig. 1. 5-phase conventional SRM with concentrated windings

The conventional 5-phase SRM having 10 stator and 8 rotor poles are shown in Fig. 1. This model has been developed in order to compare it with the designed 5-phase ST-SRM illustrated in Fig. 2. The main dimensions are similar to that designed machine of which dimensions are given in Table I.

The novel five-phase SRM design purposed includes a stator having evenly spaced salient poles and a rotor having segment type U-type cores which are embedded in aluminum block in order to increase robustness. In operation, two adjacent phases must be excited every time to create short flux loops and to provide restrained rotor rotation.

Manuscript received February 19, 2013; accepted August 28, 2013.

This research was funded by a grant (No. 07/2008-02) from Gazi University Scientific Researches Unit (BAP). It was performed in cooperation with the Institution.

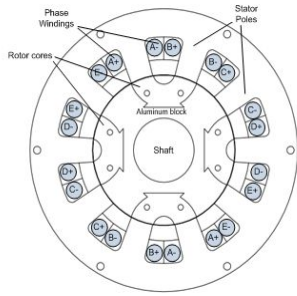


Fig. 2. 5-phase segment type SRM (ST-SRM) with concentrated windings.

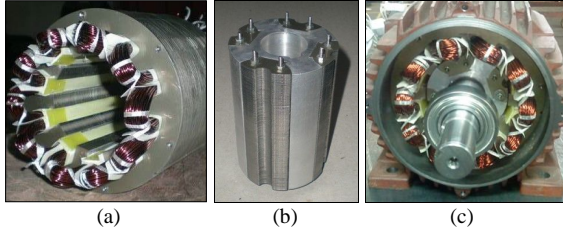


Fig. 3. Constructed machine parts: (a) Stator (b) Rotor (c) Prototype ST-SRM assembly.

TABLE I. ST-SRM'S CALCULATED AND OPTIMIZED DESIGN PARAMETERS.

No	Design Parameter	Design Value
1	Number of phases	5
2	Stator/rotor configuration	10/8
3	Stator outer diameter	150 mm
4	Rotor outer diameter	79.4 mm
5	Stack length	120 mm
6	Air gap length	0.3 mm
7	Stator pole arc	0.314 rad
8	Rotor pole arc	0.331 rad
9	Number of turns per phase	100
10	Stator/rotor construction material	M530-50A silicon steel (0.5 mm thickness)
11	Copper wire diameter	1.25 mm

As compared to designed classical SRM samples, the following merits have been aimed via this design:

- The simultaneous excitation of two phases at all times results in pairs of adjacent stator poles being magnetized with opposite polarity, thereby forming a magnetic circuit of which path includes only the portion of the yoke bridging the two adjacent stator poles of a pair.
- The produced ST-SRM significantly reduces the hysteresis and eddy current losses experienced in back iron because of the fact that the motor phases are using short flux loops all the time.
- Another specific object of the motor is to provide high torque having small torque ripple characteristics and no dead torque position for the rotor. Eventually, efficiency of the motor is increased.
- There is a gap lying along the stack length of the motor. This gap helps the motor to be cooled better.
- With this novel design, the secondary magnetic circuits causing flux switching frequency are eliminated because of the fact that only simultaneous polarized pairs are used each time.

### III. MAGNETIC CIRCUIT MODEL

#### A. Assumptions and Circuit Analysis

The magnetic equivalent circuit method, as another

approach, has been used previously to model the saturated magnetic field of SRM [5]–[7]. Some important points based upon previous work and experience gained from the FEM [8] results must be considered in order to develop an accurate and appropriate magnetic equivalent circuit model for the SRM [9]. The linear ST-SRM model is developed to show that the ST-SRM is able to produce more torque than linear conventional SRM model under the same circumstances.

During the analytical calculation and finite element method simulations, the following assumptions are taken into consideration:

- The magnetic material and current sources are ideal;
- All of the phase fluxes passing through the air gap or phase to phase leakage are assumed as “non-existing”;
- The stator back iron is infinitely permeable or  $\sim = 0$ ;
- If any of the stator poles is at unaligned position, the permeance of those phases is equal to the minimum permeance value; conversely overlapping permeance (at aligned position) gets the higher value in accordance with rotation and overlap angles.

Besides these assumptions, only two phases of the motor (e.g. Phase B and C) are deemed as being “ON” while the motor operates on simultaneous excitation of two phases at all times and thereby forming a magnetic circuit of which path includes only the portion of the yoke bridging the two adjacent stator poles of a pair. In order to express the operation difference between the conventional SRM and designed ST-SRM, the following flux distribution results derived from finite element analysis are given.

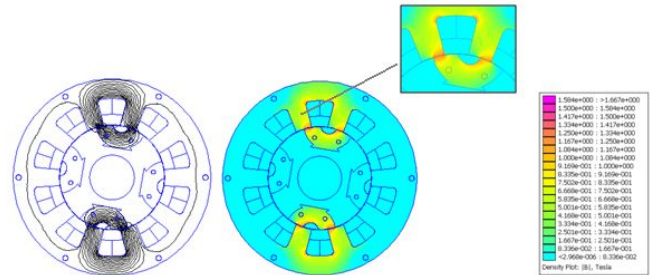


Fig. 4. Flux distributions on stator and rotor steels for 5-phase ST-SRM at semi-aligned position (a rotation of 9° over when two phases are excited simultaneously).

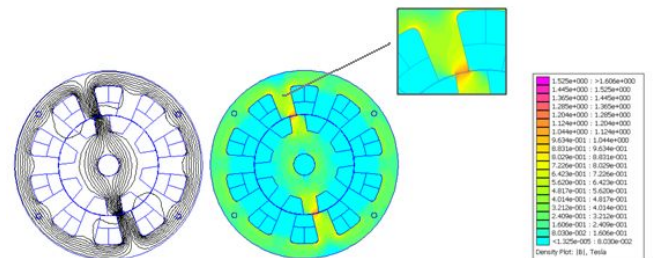


Fig. 5. Flux distributions on stator and rotor steels for 5-phase conventional SRM at semi-aligned position.

During the analyses, only one fifth of the ST-SRM is considered because of the fact that the structural geometry is repeating itself five times in polar coordinate. The flattened geometry and equivalent magnetic circuit of the ST-SRM are seen in Fig. 6 and Fig. 7 respectively.

If ST-SRM's magnetic equivalent circuit is considered,

the following equation can be written according to Kirchhoff's Laws

$$W_a + W_b + W_c + W_d + W_e = 0, \quad (1)$$

where  $w_x (x = a, b, c, d, e)$  is the phase flux. If the flux is expressed in terms of permeance

$$W_x = G_x(u_x) u_x \quad (2)$$

is obtained. While  $G_x$  is expressing the magnetic permeability (permeance),  $u_x$  expresses the MMF drop. The value of MMF sources is expressed by

$$\mathfrak{F}_x = Ni_x. \quad (3)$$

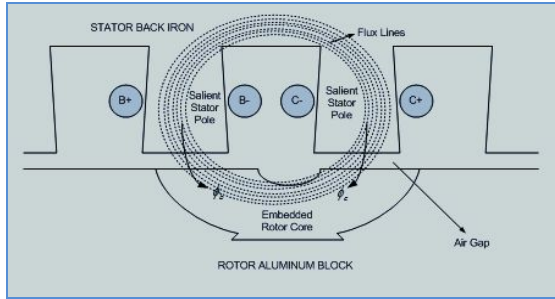


Fig. 6. Flattened stator and rotor structure of ST-SRM.

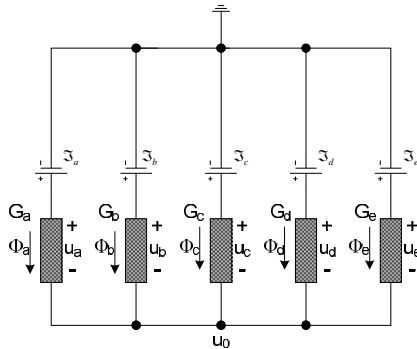


Fig. 7. Magnetic equivalent circuit for ST-SRM.

Herein,  $\mathfrak{F}_x$  gives the value of MMF source,  $N$  is the number of coils for one phase,  $i_x$  is the current value of each phase. According to the equivalent circuit, MMF drop across each reluctance path is given by

$$u_x = \mathfrak{F}_x - u_0, \quad (4)$$

where  $u_0$  is the only MMF node potential. If the expression given for phase fluxes is expanded by using the equation above

$$W_x = G_x(u_x) (\mathfrak{F}_x - u_0) \quad (5)$$

is obtained. As the flux linkage is expressed with  $\lambda = Nw$ , the flux linkage of each phase of ST-SRM can be calculated by using the expression above. Besides, the flux linkages can be also expressed via the equation below

$$\lambda_a + \lambda_b + \lambda_c + \lambda_d + \lambda_e = 0. \quad (6)$$

And the phase permeance can be written as a function of phase inductance

$$G_x = \frac{L_x}{N^2}. \quad (7)$$

If the equation is expanded by using  $\lambda = Nw$  expression

$$\lambda_x = L_x(u_x) \left( \frac{\mathfrak{F}_x - u_0}{N} \right), \quad (8)$$

is obtained. If an arbitrary current  $i_0$  is defined by using  $i_0 = \frac{u_0}{N}$ , the following flux linkage can be written

$$\lambda_x = L_x(u_x) (i_x - i_0). \quad (9)$$

If this equation is substituted in (6), this expression is obtained

$$L_a(u_x) (i_a - i_0) + L_b(u_x) (i_b - i_0) + L_c(u_x) (i_c - i_0) + L_d(u_x) (i_d - i_0) + L_e(u_x) (i_e - i_0) = 0. \quad (10)$$

If the  $i_0$  value is taken out from the equation above

$$i_0 = \frac{L_a(u_x) i_a + L_b(u_x) i_b + L_c(u_x) i_c + L_d(u_x) i_d + L_e(u_x) i_e}{L_a(u_x) + L_b(u_x) + L_c(u_x) + L_d(u_x) + L_e(u_x)} \quad (11)$$

is obtained. If the equation is arranged in accordance with (9) and (11), the flux linkage value for phase B can be obtained as

$$\lambda_b = \left( L_b(u_x) - \frac{L_b^2(u_x)}{L_a(u_x) + L_b(u_x) + L_c(u_x) + L_d(u_x) + L_e(u_x)} \right) i_b - \left( \frac{L_b(u_x) L_a(u_x) i_a + L_b(u_x) L_c(u_x) i_c + L_b(u_x) L_d(u_x) i_d + L_b(u_x) L_e(u_x) i_e}{L_a(u_x) + L_b(u_x) + L_c(u_x) + L_d(u_x) + L_e(u_x)} \right) \quad (12)$$

is obtained. From this equation, the self-inductances of the phases can be easily figured out. For instance; the self-inductance value,  $L_{bb}$  for phase B is given

$$L_{bb} = L_b(u_x) - \frac{L_b^2(u_x)}{L_a(u_x) + L_b(u_x) + L_c(u_x) + L_d(u_x) + L_e(u_x)}. \quad (13)$$

In the assumption, only two phases of the motor (herein; Phase B and Phase C) are assumed to be turned-on, so the mutual inductances between these two phases should be calculated as well. From the (12), it can also be obtained

$$M_{bc} = - \frac{L_b(u_x) L_c(u_x)}{L_a(u_x) + L_b(u_x) + L_c(u_x) + L_d(u_x) + L_e(u_x)}. \quad (14)$$

Although the other mutual inductances between other phases can be expressed mathematically in the same way, there cannot be any mutual inductance between the phases A and D and the phases B and E due to the fact that only the adjacent phases will be taken into consideration in practical

operation. In order to express these differences, the apparent inductance profiles of the motor should be examined.

For all phases, the following generalized matrices form can be used:

$$\begin{pmatrix} \lambda_a \\ \lambda_b \\ \lambda_c \\ \lambda_d \\ \lambda_e \end{pmatrix} = \begin{pmatrix} L_{aa} & M_{ab} & M_{ac} & M_{ad} & M_{ae} \\ M_{ba} & L_{bb} & M_{bc} & M_{bd} & M_{be} \\ M_{ca} & M_{cb} & L_{cc} & M_{cd} & M_{ce} \\ M_{da} & M_{db} & M_{dc} & L_{dd} & M_{de} \\ M_{ea} & M_{eb} & M_{ec} & M_{ed} & L_{ee} \end{pmatrix} \begin{pmatrix} i_a \\ i_b \\ i_c \\ i_d \\ i_e \end{pmatrix}. \quad (15)$$

### B. Apparent Inductance Profiles

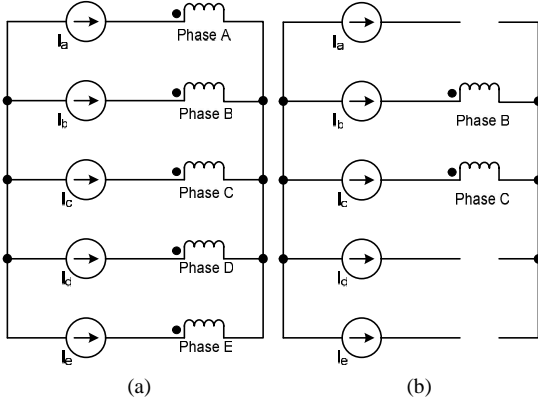


Fig. 8. (a) The equivalent circuit of ST-SRM when ideal current sources are used (b); The equivalent circuit of ST-SRM when phase B and C are excited.

Within this analytical calculation, the ST-SRM is designed with ideal current sources as seen Fig. 8(a). If only two phases of the ST-SRM are turned-on, the ST-SRM circuit becomes equivalent to the one in Fig. 8(b).

The equivalent circuit can also be expressed as in Fig. 9.

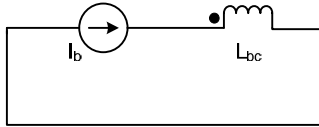


Fig. 9. Ideal equivalent circuit of ST-SRM when phase B and C are excited.

When only B and C phases are excited, the following expression can be written:

$$i_b = -i_c, \quad (16)$$

$$i_a = 0, \quad (17)$$

$$i_d = 0, \quad (18)$$

$$i_e = 0. \quad (19)$$

If the flux linkage expressions are written for these phases again:

$$\lambda_b = \left( L_b(n) - \frac{L_b^2(n)}{L_a(n) + L_b(n) + L_c(n) + L_d(n) + L_e(n)} + \frac{L_b(n)L_c(n)}{L_a(n) + L_b(n) + L_c(n) + L_d(n) + L_e(n)} \right) i_b, \quad (20)$$

$$\lambda_c = \left( L_c(n) - \frac{L_c^2(n)}{L_a(n) + L_b(n) + L_c(n) + L_d(n) + L_e(n)} + \frac{L_b(n)L_c(n)}{L_a(n) + L_b(n) + L_c(n) + L_d(n) + L_e(n)} \right) i_b. \quad (21)$$

As the value of flux linkage between these two phases is  $\lambda_{bc} = \lambda_b - \lambda_c$ , the difference between (20) and (21) becomes

$$\lambda_{bc} = \left( L_b(n) + L_c(n) - \frac{L_b^2(n) + L_c^2(n)}{L_a(n) + L_b(n) + L_c(n) + L_d(n) + L_e(n)} + \frac{2L_b(n)L_c(n)}{L_a(n) + L_b(n) + L_c(n) + L_d(n) + L_e(n)} \right) i_b. \quad (22)$$

The apparent inductance value expressed as  $L_{bc}$  can be calculated using the expression  $L = \lambda/i$

$$L_{bc} = L_b(n) + L_c(n) - \frac{L_b^2(n) + L_c^2(n)}{L_a(n) + L_b(n) + L_c(n) + L_d(n) + L_e(n)} + \frac{2L_b(n)L_c(n)}{L_a(n) + L_b(n) + L_c(n) + L_d(n) + L_e(n)}. \quad (23)$$

### C. Torque Production in ST-SRM

The co-energy which is the complementary function of magnetic field energy is expressed as the function of rotor position and excitation current as well. So, the co-energy of the motor is calculated as follow

$$W_c = \int_0^i \lambda(i, n) di. \quad (24)$$

If the matrices form in (15) is used, the expression above can be expanded as follows

$$W_c = \frac{1}{2} (L_{aa}i_a^2 + L_{bb}i_b^2 + L_{cc}i_c^2 + L_{dd}i_d^2 + L_{ee}i_e^2) + i_a i_b M_{ab} + i_a i_c M_{ac} + i_a i_d M_{ad} + i_a i_e M_{ae} + i_b i_c M_{bc} + i_b i_d M_{bd} + i_b i_e M_{be} + i_c i_d M_{cd} + i_c i_e M_{ce} + i_d i_e M_{de}. \quad (25)$$

The torque of the machine is calculated as the partial derivative of co-energy in accordance with angular position of the motor:

$$T(n, i) = -\frac{\partial W_c(n, i)}{\partial n}, \quad (26)$$

$$T = \frac{1}{2} \left( \frac{dL_{aa}}{dn} i_a^2 + \frac{dL_{bb}}{dn} i_b^2 + \frac{dL_{cc}}{dn} i_c^2 + \frac{dL_{dd}}{dn} i_d^2 + \frac{dL_{ee}}{dn} i_e^2 + i_a i_b \frac{dM_{ab}}{dn} + i_a i_c \frac{dM_{ac}}{dn} + i_a i_d \frac{dM_{ad}}{dn} + i_a i_e \frac{dM_{ae}}{dn} + i_b i_c \frac{dM_{bc}}{dn} + i_b i_d \frac{dM_{bd}}{dn} + i_b i_e \frac{dM_{be}}{dn} + i_c i_d \frac{dM_{cd}}{dn} + i_c i_e \frac{dM_{ce}}{dn} + i_d i_e \frac{dM_{de}}{dn} \right)$$

$$+i_b i_e \frac{dM_{be}}{d_n} + i_c i_d \frac{dM_{cd}}{d_n} + i_c i_e \frac{dM_{ce}}{d_n} + i_d i_e \frac{dM_{de}}{d_n}. \quad (27)$$

But, in the case that the motor is only driven under simultaneous excitation of the phases B and C and the current equation  $i_b = -i_c$  is considered, the torque equation becomes:

$$T = \frac{1}{2} \left( \frac{dL_{bb}}{d_n} i_b^2 + \frac{dL_{cc}}{d_n} i_c^2 \right) + i_b i_c \frac{dM_{bc}}{d_n}, \quad (28)$$

$$T = \frac{1}{2} \left( \frac{dL_{bb}}{d_n} i_b^2 + \frac{dL_{cc}}{d_n} i_b^2 \right) - i_b i_b \frac{dM_{bc}}{d_n}, \quad (29)$$

$$T = \left( \frac{1}{2} \left( \frac{dL_{bb}}{d_n} + \frac{dL_{cc}}{d_n} \right) - \frac{dM_{bc}}{d_n} \right) i_b^2. \quad (30)$$

#### IV. RESULTS AND DISCUSSION

Under ideal excitation, the ratio of average torque of ST-SRM to the conventional SRM is derived from simulation results. As the motor operates on simultaneous excitation of two phases at all times and thereby forming a magnetic circuit of which path includes only the portion of the yoke connecting the two adjacent stator poles of a pair, ST-SRM is able to give a higher torque output. The plot comparison is shown in Fig. 10.

Besides, the derivatives of the phase inductances with the respect to angular position are required to evaluate the torque expressions for each type of switched reluctance motor. The corresponding inductance plots are shown in Fig. 11.

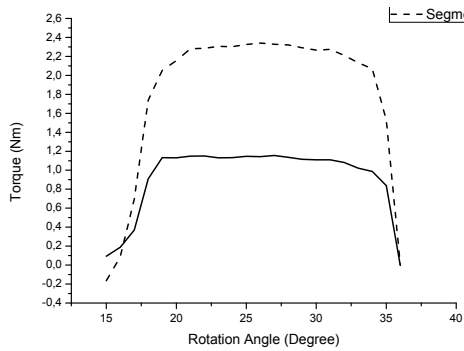


Fig. 10. Torque plots of ST-SRM and classical SRM.

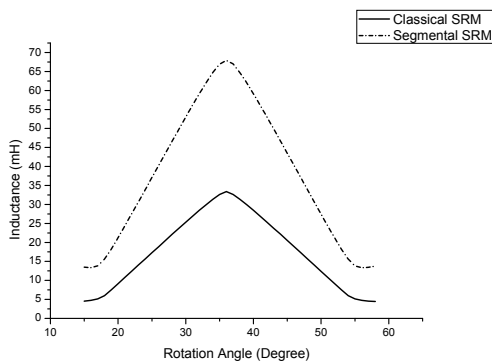


Fig. 11. Inductance plots of ST-SRM and classical SRM.

Because the models are ideal and the fringing and leakage are ignored (all of the phase fluxes passing through the air gap or phase to phase leakage are assumed as “non-

existing”) and also the unaligned permeance is constant (the stator back iron is infinitely permeable or  $\sim = 0$ ), a more complex magnetic circuit and analytical model are required for both conventional and ST-SRM. Then, the losses and torque ripples can be calculated more accurately.

#### V. CONCLUSIONS

In this study, models for a conventional 5-phase SRM and 5-phase high performance segment type SRM with U-type segment rotor cores are developed. For the similar geometry, the calculations are performed by using an equivalent magnetic circuit and underlying assumptions. The concept of apparent inductance profiles and torque equations of ST-SRM are introduced.

It is proved analytically and through finite element based studies that novel ST-SRM gives two times more torque than conventional SRM for the same input and design parameters. The summarized results which are both obtained from analytical calculations and design parameters are shown in Table II.

TABLE II. COMPARISON VARIABLES.

Parameter	Novel ST-SRM	Conventional SRM
Maximum torque at 5 A (Nm)	2.34	1.15
Active M530-50A silicon steel weight (kg)	9.90	11.47
Aluminum block weight (kg)	0.71	-
Maximum inductance (mH)	67.91	33.39
Resistance per phase (ohm)	0.56	0.56
Magnetic field energy at 5 A (Joule)	0.848	0.417
Torque/weight ratio (Nm/kg)	0.22	0.1

#### REFERENCES

- [1] J. M. Kokernak, D. A. Torrey, “Magnetic circuit model for the mutually coupled switched reluctance machine”, *IEEE Industry Applications Conf. (IAS 97)*, 1997, vol. 1, pp. 302–309.
- [2] W. Ding, D. Liang, H. Sui, “Dynamic modeling and performance prediction for dual-channel switched reluctance machine considering mutual coupling”, *IEEE Trans. on Magnetics*, vol. 46, pp. 3652–3663, 2010. [Online]. Available: <http://dx.doi.org/10.1109/TMAG.2010.2045390>
- [3] G. Bal, D. Uygun, “A Novel Switched Reluctance Motor with U-type Segmental Rotor Pairs: Design, Analysis and Simulation Results”, in *Int. Conf. Computer, Electrical, and Systems Science, and Engineering (ICCESSE 2010)*, Rome, Italy, 2010, pp. 686–690.
- [4] R. Mutlu, “Modelling of the Short Flux Path Mutually Coupled Switched Reluctance Machine”, Ph.D. dissertation, The Graduate Faculty of Rensselaer Polytechnic Institute, USA, 2004, pp. 9–18.
- [5] M. Moallem, G. E. Dawson, “An improved magnetic equivalent circuit method for predicting the characteristics of highly saturated electromagnetic devices”, *IEEE Trans. on Magnetics*, vol. 34, pp. 3632–3635, 1998. [Online]. Available: <http://dx.doi.org/10.1109/20.717858>
- [6] M. A. Preston, J. P. Lyons, “A switched reluctance motor model with mutual coupling and multi-phase excitation”, *IEEE Trans. Magnetics*, vol. 27, pp. 5423–5425, 1991. [Online]. Available: <http://dx.doi.org/10.1109/20.278859>
- [7] J. M. Kokernak, D. A. Torrey, “Magnetic circuit model for the mutually coupled switched reluctance machine”, in *IEEE IAS Annual Meeting*, 1997, vol. 1, pp. 302–309.
- [8] G. Bal, D. Uygun, “An approach to obtain an advisable ratio between stator and rotor tooth widths in switched reluctance motors for higher torque and smoother output power profile”, *Gazi University Journal of Science*, vol. 23, no. 4, pp. 457–463, 2010.
- [9] A. Deihimi, S. Farhangi, G. Henneberger, “A general nonlinear model of switched reluctance motor with mutual coupling and multiphase excitation”, *Research Journal of Electrical Engineering*, vol. 84, no. 3, pp. 143–158, July 2002. [Online]. Available: <http://dx.doi.org/10.1007/s00202-001-0113-3>